The Initial Post-buckling and Growth Behavior of Internal Delaminations in Composite Plates

G. A. Kardomateas
Assoc. Professor,
School of Aerospace Engineering,
Georgia Institute of Technology,
Atlanta, GA 30332-0150
Mem. ASME

The initial post-buckling and growth behavior of delaminations in plates is studied by a perturbation procedure. In this work, no restrictive assumptions regarding the delamination thickness and plate length are made, i.e., the usual thin film assumptions are relaxed. The perturbation procedure is based on an asymptotic expansion of the load and deformation quantities in terms of the distortion parameter of the delaminated layer, the latter being considered a compressive elastica. Closed-form solutions for the load and midpoint delamination deflection versus applied compressive displacement during the initial post-buckling phase are derived. Moreover, closed-form expressions for the energy release rate and the mixity ratio (i.e., Mode II versus Mode I) at the delamination tip are produced. A higher Mode I component is found to be present during the initial post-buckling phase for delaminations of increasing ratio of delamination thickness over plate thickness, h/T *(i.e., delaminations further away from the surface). Moreover, the energy release rate corresponding to the same applied strain is larger for a higher* h/T *ratio. The reduced growth resistance of these configurations is verified by experimental results on unidirectional composite specimens with internal delaminations.*

Introduction

Delaminations or interlayer cracks are developed as a result of imperfections in production technology or due to service loads which may include impact by foreign objects. As a consequence, structural elements with delaminations under compression suffer a degradation of their stiffness and buckling strength and potential loss of integrity from possible growth of the interlayer crack. Besides strength, delaminations can influence other performance characteristics, such as the energy absorption capacity of composite beam systems (Kardomateas and Schmueser, 1988).

Delamination buckling in plates under compression has received considerable attention and numerous contributions have addressed related issues in both one-dimensional and two-dimensional treatments (e.g., Chai et al., 1981; Simitses et al., 1985; Wang et al., 1985; Evans and Hutchinson, 1984; Chai and Babcock, 1985). However, although the critical point can be fairly well determined and has been extensively studied, limited work has focused on the post-buckling behavior, which ultimately governs the growth characteristics of the delamination.

The one configuration most thoroughly studied is the one-dimensional delamination, consisting of a delamination in an infinitely thick plate. In this model (Chai, Babcock, and Knauss, 1981), which has also been called "thin film" model, the unbuckled (base) plate is assumed to be subject to a uniform compressive strain. Closed-form expressions for the energy release rate from the thin film model were derived by Chai et al. (1981) by using the strain energy expressions before and after delamination buckling.

The other configuration most extensively studied is the axisymmetric counterpart to the one-dimensional delamination, i.e., a circular delamination in a perfectly rigid supporting plate. The latter relates also to the so-called blister test used to determine adhesive and cohesive material properties. For this configuration, Evans and Hutchinson (1984) derived a formula for the energy release rate by using an asymptotically valid solution to the system of governing equations for small buckling deflections. Results for the energy release rate of a circular delamination were also given by Chai (1990) and calculated through a path-independent integral approach by Yin (1985). In the same context, Storåkers and Andersson (1988) derived general potential energy theorems and associated bounds for composite plates within the kinematical assumptions usually attributed to von Karman, and studied in detail the efficiency of different analytical and numerical means for this circular delamination case.

For delaminations in plates that cannot fulfill the "thin

Contributed by the Applied Mechanics Division of THE AMERICAN SOCIETY OF MECHANICAL ENGINEERS for presentation at the ASME Winter Annual Meeting, New Orleans, LA, Nov. 28-Dec. 3, 1993.

Discussion on this paper should be addressed to the Technical Editor, Professor Lewis T. Wheeler, Department of Mechanical Engineering, University of Houston, Houston, TX 77204-4792, and will accepted until four months after final publication of the paper itself in the ASME JOURNAL OF APPLIED MECHANICS.

Manuscript received by the ASME Applied Mechanics Division, Aug. 10, 1992; final revision, Jan. 15, 1993. Associate Technical Editor: J. N. Reddy.

Paper No. 93-WA/APM-9.

film" model assumptions, both the critical load and the post-critical behavior are expected to deviate from the predictions of Chai et al. (1981). To this extent, Simitses et al. (1985) studied the critical load for a delamination of arbitrary thickness and size in a finite plate. Their results showed indeed a range of critical load versus thin film load ratios, depending on delamination and base plate dimensions, as well as base plate end fixity (simply supported versus clamped). Concerning the post-critical behavior of delaminations of arbitrary size, Kardomateas (1989a) provided a formulation for studying the post-buckling behavior by using elastica theory for representing the deflections of the buckled layer; this work resulted in a system of nonlinear equations rather than closed-form expressions.

In this paper, the initial post-buckling behavior of delaminated composites (with no restrictive assumptions on the delamination dimensions) is studied by using a perturbation procedure based on an asymptotic expansion of the load and deformation quantities in terms of the distortion parameter of the delaminated layer, the latter being considered a compressive elastica. The analysis will lead to closed-form solutions for the load versus applied compressive displacement and the near-tip resultant moments and forces. Subsequently, the bi-material interface crack solutions for the energy release rate and the mode mixity in terms of the resultant moments and forces, as derived by Suo and Hutchinson (1990) will be employed to study the growth characteristics of the delamination. Numerical results for a range of relative delamination thicknesses and lengths are presented and discussed. Moreover, the predicted growth characteristics are compared with experimental observations from compression tests of unidirectional composite specimens with internal debonds.

Initial Post-buckling Solution

In a delaminated system, which can be thought of as an aggregate of constitutive parts such as the delaminated layer, substrate layer, and the base plate, the conditions of geometrical continuity at the common sections (i.e., where the delamination starts or ends) play a particularly important part in the realization of equilibrium states which follow nonlinear paths. The exact laws that govern the behavior of single compressive elements elastically restrained at the ends by means of concentrated forces and moments constitutes the elastica theory (e.g., Britvek, 1973). Generalized coordinates of deformation are the distortion parameter, α, which represents the tangent rotation at an inflection point from the straight position, and the amplitude variable $\Phi(x)$. The initial post-buckling deformations are relatively small, so the exact expressions may be expanded in Taylor series in terms of the distortion parameter. Exact dependence of the end moments, end rotations, and the flexural contraction is through elliptic functions; however, the asymptotic expressions that will be given in this work are in terms of trigonometric functions.

Consider a plate of half-length L (and unit width) with a through-the-width delamination of half-length ℓ, symmetrically located (Fig. 1). The delamination is at an arbitrary position through the thickness T. Over the delaminated region, the laminate consists of the part above the delamination, of thickness h referred to as the "delaminated" part, and the part below the delamination, of thickness $H=T-h$, referred to as the "substrate" part. The remaining, intact laminate, of thickness T and length $b=L-\ell$, is referred to as the "base" plate. Without loss of generality, it may be assumed that $h<T/2$. Accordingly, the subscript $i=d, s, b$ refers to the delaminated part, the substrate or the base plate, respectively. In the following, we shall also denote by D_i the bending stiffness, $D_i=E_i t_i^3/[12(1-\nu^2)]$, t_i being the thickness of the corresponding part, E the modulus of elasticity, and ν the Poisson's ratio. For simplicity reasons, the properties of the material are assumed homogeneous, linearly elastic, and isotropic (orthotropic properties can be accounted by using $\nu_{12}\nu_{21}$ instead of ν^2 and E the modulus of elasticity along the $x=1$ axis). Notice also that in Fig. 1 the end moments and tangent rotations are assumed positive clockwise.

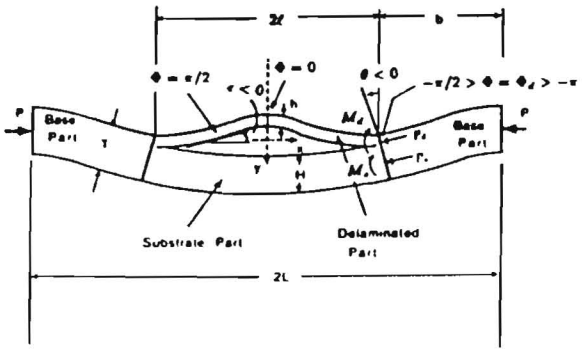

Fig. 1 Definition of the geometry

The buckled configuration of the delaminated layer is part of an inflectional elastica with end amplitude Φ_d and distortion parameter ϵ. At the critical state, the end amplitude is Φ_d^0. Suppose that in the slightly buckled configuration, Φ_d can be expanded in the form

$$\Phi_d=\Phi_d^0+\phi_d^{(1)}\epsilon+\phi_d^{(2)}\epsilon^2+O(\epsilon^3). \tag{1}$$

Then the end rotation at the common section, θ, is given by expanding the relevant expression (Britvek, 1973) in the Taylor series in terms of ϵ (notice that at the critical state $\theta^0=0$):

$$\theta=(\sin\Phi_d)\epsilon-\frac{1}{24}(\sin\Phi_d\cos^2\Phi_d)\epsilon^3+\ldots=(\sin\Phi_d^0)\epsilon$$
$$+(\cos\Phi_d^0)\phi_d^{(1)}\epsilon^2+\left[(\cos\Phi_d^0)\phi_d^{(2)}-(\sin\Phi_d^0)\frac{\phi_d^{(1)2}}{2}\right.$$
$$\left.-\frac{1}{24}\sin\Phi_d^0\cos^2\Phi_d^0\right]\epsilon^3+\ldots$$
$$=\theta^{(1)}\epsilon+\theta^{(2)}\epsilon^2+\theta^{(3)}\epsilon^3+O(\epsilon^4). \tag{2}$$

Notice that by the continuity condition, θ is the same for both the delaminated and substrate parts as well as the base plate.

The asymptotic expansion for the end moment, M_d, is similarly found by substituting (1) into the relevant expression (Britvek, 1973) and subsequently expanding in Taylor series (again $M_d^0=0$):

$$\frac{\ell M_d}{D_d}=(\Phi_d\cos\Phi_d)\epsilon+\frac{\Phi_d}{16}\left(\frac{1}{3}-\frac{\sin 2\Phi_d}{2\Phi_d}\right)(\cos\Phi_d)\epsilon^3+\ldots$$
$$=\frac{\ell}{D_d}\left(M_d^{(1)}\epsilon+M_d^{(2)}\epsilon^2+M_d^{(3)}\epsilon^3\right)+O(\epsilon^4), \tag{3a}$$

where

$$\frac{\ell M_d^{(1)}}{D_d}=\Phi_d^0\cos\Phi_d^0;\quad\frac{\ell M_d^{(2)}}{D_d}=(\cos\Phi_d^0-\Phi_d^0\sin\Phi_d^0)\phi_d^{(1)}, \tag{3b}$$

$$\frac{\ell M_d^{(3)}}{D_d}=(\cos\Phi_d^0-\Phi_d^0\sin\Phi_d^0)\phi_d^{(2)}-\left(\sin\Phi_d^0+\frac{\Phi_d^0}{2}\cos\Phi_d^0\right)\phi_d^{(1)2}$$
$$+\frac{\Phi_d^0}{16}\left(\frac{1}{3}-\frac{\sin 2\Phi_d^0}{2\Phi_d^0}\right)(\cos\Phi_d^0). \tag{3c}$$

Likewise, the axial force is given by

$$\frac{\ell^2 P_d}{D_d}=\Phi^2+\frac{\Phi^2}{8}\left(1-\frac{\sin 2\Phi}{2\Phi}\right)\epsilon^2+\ldots=\Phi_d^{02}+2\Phi_d^0\phi_d^{(1)}\epsilon$$

$$+\left[\phi_d^{(1)2}+2\Phi_d^0\phi_d^{(2)}+\frac{\Phi_d^{02}}{8}\left(1-\frac{\sin 2\Phi_d^0}{2\Phi_d^0}\right)\right]\epsilon^2+\ldots$$

$$=\frac{\ell^2}{D_d}\left(P_d^0+P_d^{(1)}\epsilon+P_d^{(2)}\epsilon^2\right)+O(\epsilon^3). \quad (4)$$

Finally, the flexural contraction, f_d, is

$$f_d=\frac{\ell}{2}\left(1-\frac{\sin 2\Phi_d}{2\Phi_d}\right)\epsilon^2+O(\epsilon^4)=\frac{\ell}{2}\left(1-\frac{\sin 2\Phi_d^0}{2\Phi_d^0}\right)\epsilon^2$$

$$+\frac{\ell}{4}\left(\frac{\sin 2\Phi_d^0}{\Phi_d^0}-\frac{2\cos 2\Phi_d^{02}}{\Phi_d^0}\right)\phi_d^{(1)}\epsilon^3+\ldots=f_d^{(2)}\epsilon^2+f_d^{(3)}\epsilon^3+O(\epsilon^4). \quad (5)$$

Although the substrate part and the base plate undergo moderate bending with no inflection point, we may also use the elastic theory to describe their (nonlinear) deformation; in this case the inflection points are outside the actual elastic curve. For the substrate part, we have to expand not only the amplitude Φ_s, but also the distortion parameter α_s in a perturbation series with respect to the distortion parameter of the delamination layer ϵ:

$$\Phi_s=\Phi_s^0+\phi_s^{(1)}\epsilon+\phi_s^{(2)}\epsilon^2+O(\epsilon^3), \quad (6a)$$

$$\alpha_s=\alpha_s^{(1)}\epsilon+\alpha_s^{(2)}\epsilon^2+\alpha_s^{(3)}\epsilon^3+O(\epsilon^4). \quad (6b)$$

Then the end rotation at the common section θ is given by expanding again in Taylor series in terms of ϵ:

$$\theta=(\sin\Phi_s)\alpha_s-\frac{1}{24}(\sin\Phi_s\cos^2\Phi_s)\alpha_s^3+\ldots$$

$$=\theta_s^{(1)}\epsilon+\theta_s^{(2)}\epsilon^2+\theta_s^{(3)}\epsilon^3+O(\epsilon^4), \quad (7a)$$

where

$$\theta_s^{(1)}=(\sin\Phi_s^0)\alpha_s^{(1)};\quad \theta_s^{(2)}=(\cos\Phi_s^0)\phi_s^{(1)}\alpha_s^{(1)}+(\sin\Phi_s^0)\alpha_s^{(2)}, \quad (7b)$$

$$\theta_s^{(3)}=\left[(\cos\Phi_s^0)\phi_s^{(2)}-(\sin\Phi_s^0)\frac{\phi_s^{(1)2}}{2}\right]\alpha_s^{(1)}+(\cos\Phi_s^0)\phi_s^{(1)}\alpha_s^{(2)}$$

$$+(\sin\Phi_s^0)\alpha_s^{(3)}-\frac{1}{24}\sin\Phi_s^0\cos^2\Phi_s^0\alpha_s^{(1)3}. \quad (7c)$$

In a similar fashion, by using the expressions (6), the asymptotic expansion for the end moment, M_s is (again $M_s^0=0$):

$$\frac{\ell M_s}{D_s}=(\Phi_s\cos\Phi_s)\alpha_s+\frac{\Phi_s}{16}\left(\frac{1}{3}-\frac{\sin 2\Phi_s}{2\Phi_s}\right)(\cos\Phi_s)\alpha_s^3+\ldots$$

$$=\frac{\ell}{D_s}\left(M_s^{(1)}\epsilon+M_s^{(2)}\epsilon^2+M_s^{(3)}\epsilon^3\right)+O(\epsilon^4), \quad (8a)$$

where

$$\frac{\ell M_s^{(1)}}{D_s}=(\Phi_s^0\cos\Phi_s^0)\alpha_s^{(1)}, \quad (8b)$$

$$\frac{\ell M_s^{(2)}}{D_s}=(\cos\Phi_s^0-\Phi_s^0\sin\Phi_s^0)\phi_s^{(1)}\alpha_s^{(1)}+(\Phi_s^0\cos\Phi_s^0)\alpha_s^{(2)}, \quad (8c)$$

$$\frac{\ell M_s^{(3)}}{D_s}=(\Phi_s^0\cos\Phi_s^0)\alpha_s^{(3)}+(\cos\Phi_s^0-\Phi_s^0\sin\Phi_s^0)(\phi_s^{(2)}\alpha_s^{(1)}+\phi_s^{(1)}\alpha_s^{(2)})$$

$$-\left(\sin\Phi_s^0+\frac{\Phi_s^0}{2}\cos\Phi_s^0\right)\phi_s^{(1)2}\alpha_s^{(1)}$$

$$+\frac{\Phi_s^0}{16}\left(\frac{1}{3}-\frac{\sin 2\Phi_s^0}{2\Phi_s^0}\right)(\cos\Phi_s^0)\alpha_s^{(1)3}. \quad (8d)$$

Likewise, the axial force is given by

$$\frac{\ell^2 P_s}{D_s}=\Phi_s^2+\frac{\Phi_s^2}{8}\left(1-\frac{\sin 2\Phi_s}{2\Phi_s}\right)\epsilon^2+\ldots$$

$$=\frac{\ell^2}{D_s}\left(P_s^0+P_s^{(1)}\epsilon+P_s^{(2)}\epsilon^2\right)+O(\epsilon^3), \quad (9a)$$

where

$$\frac{\ell^2 P_s^0}{D_s}=\Phi_s^{02};\qquad \frac{\ell^2 P_s^{(1)}}{D_s}=2\Phi_s^0\phi_s^{(1)}, \quad (9b)$$

$$\frac{\ell^2 P_s^{(2)}}{D_s}=\phi_s^{(1)2}+2\Phi_s^0\phi_s^{(2)}+\frac{\Phi_s^{02}}{8}\left(1-\frac{\sin 2\Phi_s^0}{2\Phi_s^0}\right)\alpha_s^{(1)2}. \quad (9c)$$

Finally, the asymptotic expansion for the flexural contraction, f_s, is found to be

$$f_s=\frac{\ell}{2}\left(1-\frac{\sin 2\Phi_s}{2\Phi_s}\right)\alpha_s^2+O(\alpha_s^4)$$

$$=f_s^{(2)}\epsilon^2+f_s^{(3)}\epsilon^3+O(\epsilon^4), \quad (10a)$$

where

$$f_s^{(2)}=\frac{\ell}{2}\left(1-\frac{\sin 2\Phi_s^0}{2\Phi_s^0}\right)\alpha_s^{(1)2}, \quad (10b)$$

$$f_s^{(3)}=\frac{\ell}{4}\left(\frac{\sin 2\Phi_s^0}{\Phi_s^{02}}-\frac{2\cos 2\Phi_s^0}{\Phi_s^0}\right)\phi_s^{(1)}\alpha_s^{(1)2}$$

$$+\ell\left(1-\frac{\sin 2\Phi_s^0}{2\Phi_s^0}\right)\alpha^{(1)}\alpha_s^{(2)}. \quad (10c)$$

The base plate is assumed to be simply supported, so at the simply supported end, the amplitude $\Phi=-\pi/2$ and at the common section $\Phi=\Phi_b$. The amplitude at the common section and the distortion parameter of the base plate are now expanded in terms of the distortion parameter of the delaminated part ϵ:

$$\Phi_b=\Phi_b^0+\phi_b^{(1)}\epsilon+\phi_b^{(2)}\epsilon^2+O(\epsilon^3), \quad (11a)$$

$$\alpha_b=\alpha_b^{(1)}\epsilon+\alpha_b^{(2)}\epsilon^2+\alpha_b^{(3)}\epsilon^3+O(\epsilon^4). \quad (11b)$$

Moreover, the end rotation at the common section θ is given by expanding again the relevant expression from Britvek (1973) in Taylor series in terms of ϵ:

$$\theta=\left[\sin\Phi_b+\frac{\cos\Phi_b}{\Phi_b+(\pi/2)}\right]\alpha_b+R(\Phi_b)\alpha_b^3+\ldots$$

$$=\theta_b^{(1)}\epsilon+\theta_b^{(2)}\epsilon^2+\theta_b^{(3)}\epsilon^3+O(\epsilon^4), \quad (12a)$$

where $R(\Phi_b)$ is defined by

$$R(\Phi_b)=\frac{7}{48}\frac{\cos\Phi_b}{\Phi_b+(\pi/2)}-\frac{3}{32}\frac{\cos\Phi_b\sin 2\Phi_b}{[\Phi_b+(\pi/2)]^2}-\frac{1}{3}\frac{\cos^3\Phi_b}{[\Phi_b+(\pi/2)]^3}$$

$$-\frac{1}{24}\sin\Phi_b\cos^2\Phi_b. \quad (12b)$$

In terms of

$$\beta=\sin\Phi_b^0-\frac{\cos\Phi_b^0}{\Phi_b^0+(\pi/2)};\quad q=\cos\Phi_b^0-\left(\Phi_b^0+\frac{\pi}{2}\right)\sin\Phi_b^0, \quad (12c)$$

$$\xi=\cos\Phi_b^0-\frac{\sin\Phi_b^0}{\Phi_b^0+(\pi/2)}-\frac{\cos\Phi_b^0}{[\Phi_b^0+(\pi/2)]^2}, \quad (12d)$$

$$\chi=\frac{\cos\Phi_b^0}{[\Phi_b^0+(\pi/2)]^3)}+\frac{\sin\Phi_b^0}{[\Phi_b^0+(\pi/2)]^2}-\frac{\cos\Phi_b^0}{2[\Phi_b^0+(\pi/2)]}-\frac{\sin\Phi_b^0}{2}, \quad (12e)$$

we obtain

$$\theta_b^{(1)}=\beta\alpha_b^{(1)};\quad \theta_b^{(2)}=\xi\phi_b^{(1)}\alpha_b^{(1)}+\beta\alpha_b^{(2)}, \quad (12f)$$

$$\theta_b^{(3)}=\beta\alpha_b^{(3)}+\xi[\phi_b^{(1)}\alpha_b^{(2)}+\phi_b^{(2)}\alpha_b^{(1)}]$$

$$+\chi\phi_b^{(1)2}\alpha_b^{(1)}+R(\Phi_b^0)\alpha_b^{(1)3}. \quad (12g)$$

Concerning the end moment, M_b, use of (11) gives the following asymptotic expansion (again $M_b^0=0$):

$$\frac{bM_b}{D_b}=\left(\Phi_b+\frac{\pi}{2}\right)(\cos\Phi_b)\alpha_b+\frac{1}{16}\left(\Phi_b+\frac{\pi}{2}\right)$$

$$\times\left(\frac{1}{3}-\frac{\sin 2\Phi_b}{2[\Phi_b^0+(\pi/2)]}\right)(\cos\Phi_b)\alpha_b^3+\ldots$$

$$=\frac{b}{D_b}\left(M_b^{(1)}\epsilon+M_b^{(2)}\epsilon^2+M_b^{(3)}\epsilon^3\right)+O(\epsilon^4), \quad (13a)$$

where

$$\frac{bM_b^{(1)}}{D_b}=\left(\Phi_b^0+\frac{\pi}{2}\right)(\cos\Phi_b^0)\alpha_b^{(1)}, \quad (13b)$$

$$\frac{bM_b^{(2)}}{D_b}=q\phi_b^{(1)}\alpha_b^{(1)}+\left(\Phi_b^0+\frac{\pi}{2}\right)(\cos\Phi_b^0)\alpha_b^{(2)}, \quad (13c)$$

$$\frac{bM_b^{(3)}}{D_b}=\left(\Phi_b^0+\frac{\pi}{2}\right)(\cos\Phi_b^0)\alpha_b^{(3)}$$

$$-\left[\sin\Phi_b^0+\left(\Phi_b^0+\frac{\pi}{2}\right)\frac{\cos\Phi_b^0}{2}\right]\phi_b^{(1)2}\alpha_b^{(1)}+q(\alpha_b^{(1)}\alpha_b^{(2)}+\phi_b^{(2)}\alpha_b^{(1)})$$

$$+\frac{1}{16}\left(\Phi_b^0+\frac{\pi}{2}\right)\left(\frac{1}{3}-\frac{\sin 2\Phi_b^0}{2[\Phi_b^0+(\pi/2)]}\right)(\cos\Phi_b^0)\alpha_b^{(1)3}. \quad (13d)$$

Likewise, the axial force at the base plate (which is also the applied force) is given by

$$\frac{b^2P}{D_p}=\left(\Phi_b+\frac{\pi}{2}\right)^2+\left(\Phi_b+\frac{\pi}{2}\right)^2\left[\frac{1}{8}-\frac{1}{16}\frac{\sin 2\Phi_b}{[\Phi_b+(\pi/2)]}\right.$$

$$\left.-\frac{1}{2}\frac{\cos^2\Phi_b}{[\Phi_b+(\pi/2)]^2}\right]\alpha_b^2=\frac{b^2}{D_b}\left(P^0+P^{(1)}\epsilon+P^{(2)}\epsilon^2\right)+O(\epsilon^3), \quad (14a)$$

where

$$\frac{b^2P^0}{D_b}=\left(\Phi_b^0+\frac{\pi}{2}\right)^2; \quad \frac{b^2P^{(1)}}{D_b}=2\left(\Phi_b^0+\frac{\pi}{2}\right)\phi_b^{(1)}, \quad (14b)$$

$$\frac{b^2P^{(2)}}{D_b}=\phi_b^{(1)2}+2\left(\Phi_b^0+\frac{\pi}{2}\right)\phi_b^{(2)}$$

$$+\frac{1}{8}\left(\Phi_b^0+\frac{\pi}{2}\right)^2\left[1-\frac{\sin 2\Phi_b^0}{2[\Phi_b^0+(\pi/2)]}-\frac{4\cos^2\Phi_b^0}{[\Phi_b^0+(\pi/2)]^2}\right]\alpha_b^{(1)2}. \quad (14c)$$

Finally, the flexural contraction, f_b, between the simply supported end and the common section is

$$f=\frac{b}{4}\left[1-\frac{\sin 2\Phi_b}{2[\Phi_b+(\pi/2)]}-\frac{2\cos^2\Phi_b}{[\Phi_b+(\pi/2)]^2}\right]\alpha_b^2+\ldots$$

$$=f_b^{(2)}\epsilon^2+O(\epsilon^3), \quad (15a)$$

where

$$f_b^{(2)}=\frac{b}{4}\left[1-\frac{\sin 2\Phi_b^0}{2[\Phi_b^0+(\pi/2)]}-\frac{2\cos^2\Phi_b^0}{[\Phi_b^0+(\pi/2)]^2}\right]\alpha_b^{(1)2}. \quad (15b)$$

Having obtained the asymptotic expressions for the force and deformation quantities, we shall discuss the formulation of the equilibrium and compatibility requirements that will ultimately define the nonlinear post-critical path. Force and moment equilibrium at the common section require

$$P_d+P_s-P=0, \quad (16a)$$

$$M_d+M_s+M_b-P_d\frac{H}{2}+P_s\frac{h}{2}=0. \quad (16b)$$

The deflections of the delaminated and substrate parts should be geometrically compatible. Thus, a second condition necessary for a solution involves the compatible shortening of the delaminated and substrate parts, which consists, in turn, of the compressive and flexural shortening:

$$\left(f_d+2\frac{P_d\ell}{Eh}\right)-\left(f_s+2\frac{P_s\ell}{EH}\right)+\theta T=0. \quad (17)$$

As the compressive load P is applied, the plate remains flat and a primary state solution (pure compression) is characterized by $P^0=P_d^0T/h$ and $P_s^0=P_d^0H/h$, which gives

$$\Phi_s^0=\Phi_d^0\sqrt{\frac{D_dH}{D_sh}}; \quad \Phi_b^0=-\Phi_d^0\frac{b}{\ell}\sqrt{\frac{D_dT}{D_bh}}-\pi/2. \quad (18a)$$

Although determination of the critical point is not a primary objective of this paper and the buckling analysis has been thoroughly carried out in other works (e.g., Simitses et al., 1985), we shall briefly describe the equations for the critical point (in terms of Φ_d^0) for the sake of completeness, and because the formulation for the initial post-buckling naturally follows that for the critical point.

By equating the first-order rotation at the common section we obtain $\alpha_s^{(1)}$ and $\alpha_b^{(1)}$:

$$\alpha_s^{(1)}=\frac{\sin\Phi_d^0}{\sin\Phi_s^0}; \quad \alpha_b^{(1)}=\frac{\sin\Phi_d^0}{\beta}. \quad (18b)$$

Writing the moment equilibrium (16*b*) and the geometric compatibility (17) for the first-order terms and eliminating the quantity $[P_d^{(1)}H-P_s^{(1)}h]$ leads to the characteristic equation, for the determination of Φ_d^0:

$$\frac{D_d}{\ell}\Phi_d^0\cos\Phi_d^0+\sin\Phi_d^0\left[\frac{D_s}{\ell}\Phi_s^0\cot\Phi_s^0\right.$$

$$\left.+\frac{D_b}{b}\left(\Phi_b^0+\frac{\pi}{2}\right)\frac{\cos\Phi_b^0}{\beta}+\frac{EThH}{4\ell}\right]=0. \quad (18c)$$

Next, the initial post-buckling behavior is considered.

First-Order Forces. Force equilibrium, Eq. (16*a*) for the first-order terms, and use of (4), (9*b*), and (14*b*) for the first-order forces gives

$$\phi_b^{(1)}=\frac{\Phi_d^0}{\Phi_b^0+(\pi/2)}\frac{D_db^2}{D_b\ell^2}\phi_d^{(1)}+\frac{\Phi_s^0}{\Phi_b^0+(\pi/2)}\frac{D_sb^2}{D_b\ell^2}\phi_s^{(1)}$$

$$=\rho_d\phi_d^{(1)}+\rho_s\phi_s^{(1)}. \quad (19a)$$

By equating the second-order terms in the expressions for the slope at the common section, $\theta^{(2)}$, Eqs. (2), (7*b*), and (12*f*) we can find $\alpha_s^{(2)}$ and $\alpha_b^{(2)}$ as follows:

$$\alpha_s^{(2)}=\frac{\cos\Phi_d^0}{\sin\Phi_s^0}\phi_d^{(1)}-\frac{(\cos\Phi_s^0)\alpha_s^{(1)}}{\sin\Phi_s^0}\phi_s^{(1)}=\gamma_d\phi_d^{(1)}+\phi_s\phi_s^{(1)}, \quad (19b)$$

$$\alpha_b^{(2)}=\frac{\cos\Phi_d^0}{\beta}\phi_d^{(1)}-\frac{\xi\alpha_b^{(1)}}{\beta}\phi_b^{(1)}. \quad (19c)$$

Using (19*a*) we can write $\alpha_b^{(2)}$ in the form

$$\alpha_b^{(2)}=\eta_d\phi_d^{(1)}+\eta_s\phi_s^{(1)}, \quad (19d)$$

where

$$\eta_d=\frac{\cos\Phi_d^0}{\beta}-\frac{\xi\alpha_b^{(1)}}{\beta}\rho_d; \quad \eta_s=-\frac{\xi\alpha_b^{(1)}}{\beta}\rho_s. \quad (19e)$$

Determination of the first-order forces requires deriving $\phi_d^{(1)}$ and $\phi_s^{(1)}$ and this will be discussed next. The moment equilibrium Eq. (16*b*) for the second-order terms is

$$M_d^{(2)}+M_s^{(2)}+M_b^{(2)}=\frac{1}{2}\left[P_d^{(2)}H-P_s^{(2)}h\right]. \quad (20)$$

The geometric compatibility Eq. (17) for the second-order terms gives

$$f_d^{(2)}-f_s^{(2)}+\theta^{(2)}T=\left[P_s^{(2)}h-P_d^{(2)}H\right]\frac{2\ell}{EhH}. \quad (21)$$

Eliminating the quantity $[P_s^{(2)}h-P_d^{(2)}H]$ from Eqs. (20) and (21) gives the following first linear equation for $\phi_d^{(1)}$ and $\phi_s^{(1)}$:

$$a_{11}\phi_d^{(1)}+a_{12}\phi_s^{(1)}=\left[\frac{\ell}{2}\left(1-\frac{\sin 2\Phi_s^0}{2\Phi_s^0}\right)\alpha_s^{(1)2}\right.$$

$$\left.-\frac{\ell}{2}\left(1-\frac{\sin 2\Phi_d^0}{2\Phi_d^0}\right)\right]\frac{EhH}{4\ell}, \quad (22a)$$

where

$$a_{11}=\frac{D_d}{\ell}(\cos\Phi_d^0-\Phi_d^0\sin\Phi_d^0)+\frac{D_s}{\ell}\Phi_s^0(\cos\Phi_s^0)\gamma_d+(\cos\Phi_d^0)$$
$$\times\frac{EhHT}{4\ell}+\frac{D_b}{b}\left[q\alpha_b^{(1)}\rho_d+\left(\Phi_b^0+\frac{\pi}{2}\right)(\cos\Phi_b^0)\eta_d\right]. \quad (22b)$$

$$a_{12}=\frac{D_s}{\ell}(\cos\Phi_s^0-\Phi_s^0\sin\Phi_s^0)\alpha_s^{(1)}+\Phi_s^0(\cos\Phi_s^0)\gamma_s$$
$$+\frac{D_b}{b}\left[q\alpha_b^{(1)}\rho_s+\left(\Phi_b^0+\frac{\pi}{2}\right)(\cos\Phi_b^0)\eta_s\right]. \quad (22c)$$

The second equation needed to find $\phi_d^{(1)}$ and $\phi_s^{(1)}$ is the first-order geometric compatibility Eq. (17) at the common section, which becomes after the expressions (4) and (9*b*) for the first-order delamination and substrate forces, and (2) for the first-order rotation, are substituted:

$$\frac{D_s}{\ell^2}\Phi_s^0 h\phi_s^{(1)}-\frac{D_d}{\ell^2}\Phi_d^0 H\phi_d^{(1)}=\frac{EhHT}{4\ell}\sin\Phi_d^0. \quad (23)$$

The foregoing system of two linear Eqs., (22*a*) and (23), allows finding $\phi_d^{(1)}$ and $\phi_s^{(1)}$, and hence the first-order forces $P_d^{(1)}$, $P_s^{(1)}$ and the first-order applied force $P^{(1)}=P_d^{(1)}+P_s^{(1)}$.

Second-Order Forces. Second-order force equilibrium (16*a*), together with (4), (9*c*), and (14*c*), gives

$$\phi_b^{(2)}=\rho_d\phi_d^{(2)}+\rho_s\phi_s^{(2)}+\rho_c, \quad (24a)$$

where

$$\rho_c=\rho_d\left[\frac{\phi_d^{(1)2}}{2\Phi_d^0}+\frac{\Phi_d^0}{16}\left(1-\frac{\sin 2\Phi_d^0}{2\Phi_d^0}\right)\right]$$
$$+\rho_s\left[\frac{\phi_s^{(1)2}}{2\Phi_s^0}+\frac{\Phi_s^0}{16}\left(1-\frac{\sin 2\Phi_s^0}{2\Phi_s^0}\right)\alpha_s^{(1)2}\right]-\frac{\phi_b^{(1)2}}{2[\Phi_b^0+(\pi/2)]}$$
$$-\frac{1}{16}\left(\Phi_b^0+\frac{\pi}{2}\right)\left[1-\frac{\sin 2\Phi_b^0}{2[\Phi_b^0+(\pi/2)]}-\frac{4\cos^2\Phi_b^0}{[\Phi_b^0+(\pi/2)]^2}\right]\alpha_b^{(1)2}. \quad (24b)$$

By equating the third-order terms in the expressions for the slope at the common section for the delaminated and the substrate parts, $\theta^{(3)}$, Eqs. (2) and (7*c*), we can find $\alpha_s^{(3)}$,

$$\alpha_s^{(3)}=\gamma_d\phi_d^{(2)}+\gamma_s\phi_s^{(2)}+\gamma_c, \quad (25a)$$

where γ_c is given in terms of the following quantities:

$$\psi_d=-\left(\frac{\phi_d^{(1)2}}{2}+\frac{1}{24}\cos^2\Phi_d^0\right)\sin\Phi_d^0, \quad (25b)$$

$$\psi_s=-\left(\frac{\phi_s^{(1)2}}{2}+\frac{1}{24}\alpha_s^{(1)2}\cos^2\Phi_s^0\right)\alpha_s^{(1)}\sin\Phi_s^0$$
$$+\phi_s^{(1)}\alpha_s^{(2)}\cos\Phi_s^0 \quad (25c)$$

as follows:

$$\gamma_c=\frac{\psi_d-\psi_s}{\sin\Phi_s^0}. \quad (25d)$$

In a similar fashion, by equating the third-order terms in the expressions for the slope at the common section for the delaminated and the base parts, and using (24*a*) we can write $\alpha_b^{(3)}$ in the form

$$\alpha_b^{(3)}=\eta_d\phi_d^{(2)}+\eta_s\phi_s^{(2)}+\eta_c, \quad (26a)$$

where

$$\beta\eta_c=\psi_d-(\xi\rho_c+\chi)\alpha_b^{(1)}-\xi\phi_b^{(1)}\alpha_b^{(2)}-R(\Phi_b^0)\alpha_b^{(1)3}. \quad (26b)$$

Determination of the second-order forces requires deriving $\sigma_d^{(2)}$ and $\sigma_s^{(2)}$ and this will be discussed next. The moment equilibrium Eq. (16*b*) for the third-order terms is

$$M_d^{(3)}+M_s^{(3)}+M_b^{(3)}=\frac{1}{2}[P_d^{(3)}H-P_s^{(3)}h]. \quad (27a)$$

The geometric compatibility Eq. (17) for the third-order terms gives

$$f_d^{(3)}-f_s^{(3)}+\theta^{(3)}T=[P_s^{(3)}h-P_d^{(3)}H]\frac{2\ell}{EhH}. \quad (27b)$$

Eliminating now the quantity $[P_s^{(3)}h-P_d^{(3)}H]$ from Eqs. (27*a*) and (27*b*) gives the following first linear equation for $\phi_d^{(2)}$ and $\phi_s^{(2)}$:

$$a_{11}\phi_d^{(2)}+a_{12}\phi_s^{(2)}=c_1, \quad (28)$$

where the coefficients a_{11} and a_{12} are the same as in the first-order problem, Eqs. (22*b*, *c*), and c_1 is given in Appendix A.

The second equation needed to find $\phi_d^{(2)}$ and $\phi_s^{(2)}$ is the second-order geometric compatibility Eq. (17) at the common section, which becomes after the expressions (4) and (9*c*) for the second-order forces, and (2) for the second-order rotation, are substituted:

$$\frac{D_s}{\ell^2}\Phi_s^0 h\phi_s^{(2)}-\frac{D_d}{\ell^2}\Phi_d^0 H\phi_d^{(2)}=\left[1-\frac{\sin 2\Phi_d^0}{2\Phi_d^0}-\left(1-\frac{\sin 2\Phi_s^0}{2\Phi_s^0}\right)\alpha_s^{(1)2}\right.$$
$$\left.+\frac{2T}{\ell}\phi_d^{(1)}\cos\Phi_d^0\right]\frac{EhH}{8}+\left[\phi_d^{(1)2}+\frac{\Phi_d^{02}}{8}\left(1-\frac{\sin 2\Phi_d^0}{2\Phi_d^0}\right)\right]\frac{D_dH}{2\ell^2}$$
$$-\left[\phi_s^{(1)2}+\frac{\Phi_s^{02}}{8}\left(1-\frac{\sin 2\Phi_s^0}{2\Phi_s^0}\right)\alpha_s^{(1)2}\right]\frac{D_sh}{2\ell^2}. \quad (29)$$

The foregoing system of two linear Eqs. (28) and (29) allows finding $\phi_d^{(2)}$ and $\phi_s^{(2)}$, and hence the second-order forces $P_d^{(2)}$, $P_s^{(2)}$ and the second-order applied force $P^{(2)}=P_d^{(2)}+P_s^{(2)}$.

Displacements. Next we shall discuss the expressions during the initial post-buckling stage for two additional quantities, which are typically needed for correlation with experimental data: the midpoint deflection of the delaminated layer and the substrate part, and the applied compressive displacement (or applied strain).

First, it should be noted that at each point x there corresponds a value of the variable amplitude $\Phi(x)$; the value at the common section $x=\ell$ is Φ_i, $i=d, s$. Furthermore, at the midpoint $x=0$, where the slope is zero, $\Phi=0$ and at the inflection point, where the slope is α_i, $\Phi=\pi/2$. The deflection increment on the elastica is given by (Britvek, 1973)

$$dw_i=2\sin\left(\frac{\alpha_i}{2}\right)\sqrt{\frac{D_d}{P_d}}\sin\Phi d\Phi. \quad (30a)$$

Integrating between the midpoint ($x=0$) and the common interface ($x=\ell$) gives the midpoint deflection

$$w_{im}=2\sin\left(\frac{\alpha_i}{2}\right)\sqrt{\frac{D_d}{P_d}}(\cos\Phi_i-1). \quad (30b)$$

Substituting the asymptotic expansions for the force P_i and for the amplitude Φ_i, gives the midpoint displacement of the delaminated layer or the substrate part ($i=d, s$) as follows:

$$w_{im}=w_{im}^{(1)}\epsilon+w_{im}^{(2)}\epsilon^2+\ldots, \quad (31a)$$

where for the delaminated layer

$$w_{dm}^{(1)}=\frac{\ell}{\Phi_d^0}(\cos\Phi_d^0-1), \quad (31b)$$

$$w_{dm}^{(2)}=\frac{\ell}{\Phi_d^0}\left[\frac{(1-\cos\Phi_d^0)}{\Phi_d^0}-\sin\Phi_d^0\right]\phi_d^{(1)}, \quad (31c)$$

and for the substrate part after substitution of (6*b*),

$$w_{sm}^{(1)}\frac{\Phi_i^0}{\ell}=(\cos\Phi_s^0-1)\alpha_s^{(1)}, \quad (31d)$$

$$w_{sm}^{(2)}\frac{\Phi_i^0}{\ell}=\left[\frac{(1-\cos\Phi_s^0)}{\Phi_s^0}-\sin\Phi_s^0\right]\phi_s^{(1)}\alpha_s^{(1)} \quad (31e)$$
$$+(\cos\Phi_s^0-1)\alpha_s^{(2)}. \quad (31e)$$

Finally, the previous analysis allows finding a direct expression for the applied strain, ϵ_0, as follows:

$$\epsilon_0 L = \frac{P^0 L}{ET} + \left[\frac{P^{(1)}b}{ET} + \frac{P_d^{(1)}\ell}{Eh} + \frac{H}{2}\theta^{(1)}\right]\epsilon + \left[\frac{f_d^{(2)}}{2} + \frac{P_d^{(2)}\ell}{Eh} + f_b^{(2)} + \frac{P^{(2)}b}{ET} + \frac{H}{2}\theta^{(2)}\right]\epsilon^2 + \ldots \quad (32)$$

Delamination Growth Characteristics

Before applying the initial post-buckling solution that has just been presented, the basic interface crack solutions that are needed in the analysis will be reviewed. For a general bimaterial interface crack, these solutions depend on the Dundurs (1969) parameters, $\tilde{\alpha}$, $\tilde{\beta}$ and the bimaterial constant $\tilde{\epsilon}$. For the homogeneous system under consideration, $\tilde{\alpha} = \tilde{\beta} = \tilde{\epsilon} = 0$. Therefore, the formulas of Suo and Hutchinson (1990) will be presented with the homogeneous material assumption into consideration.

For the plane-strain interface crack shown in Fig. 1, the energy release rate G is

$$G = \frac{1-\nu}{4\mu}\left[\frac{P^{*2}}{Ah} + \frac{M^{*2}}{Ih^3} + 2\frac{P^*M^*}{\sqrt{AI}h^2}\sin\gamma\right] \quad (33)$$

where μ is the shear modulus. In terms of

$$\eta = h/H;\ C_1 = \frac{h}{T};\ C_2 = \frac{6h^2H}{T^3};\ C_3 = \frac{h^3}{T^3} \quad (34)$$

P^* and M^* are linear combinations of the loads from the previous post-buckling solution:

$$P^* = P_d - C_1 P - C_2\frac{M_b}{h}, \quad (35a)$$

$$M^* = M_d - C_3 M_b. \quad (35b)$$

Moreover, A and I are positive dimensionless numbers and the angle γ is restricted such that $\gamma \le \pi/2$. These quantities are given by

$$A = \frac{1}{1+4\eta+6\eta^2+3\eta^3};\ I = \frac{1}{12(1+\eta^3)};\ \sin\gamma = 6\eta^2(1+\eta)\sqrt{AI}. \quad (36)$$

The preceding formula does not separate the opening and shearing components. Instead, the following two expressions give the Mode I and Mode II stress intensity factors

$$K_I = \frac{1}{\sqrt{2}}\left[\frac{P^*}{\sqrt{Ah}}\cos\omega + \frac{M^*}{\sqrt{Ih^3}}\sin(\omega+\gamma)\right] \quad (37a)$$

$$K_{II} = \frac{1}{\sqrt{2}}\left[\frac{P^*}{\sqrt{Ah}}\sin\omega - \frac{M^*}{\sqrt{Ih^3}}\cos(\omega+\gamma)\right]. \quad (37b)$$

Accurate determination of ω, which depends only on η (for a fixed set of Dundurs constants $\tilde{\alpha}$, $\tilde{\beta}$), requires the numerical solution of an integral equation and has been reported in Suo and Hutchinson (1990). The extracted ω, however, varies slowly with η in the entire range $0 \le \eta \le 1$, in accordance with the approximate formula (Hutchinson and Suo, 1991)

$$\omega = 52.1^0 - 3^0\eta. \quad (38)$$

The mode mixity is defined by

$$\psi = \tan^{-1}(K_{II}/K_I) = \tan^{-1}\left[\frac{\lambda\sin\omega - \cos(\omega+\gamma)}{\lambda\cos\omega + \sin(\omega+\gamma)}\right], \quad (39a)$$

where λ measures the loading combination as

$$\lambda = \sqrt{\frac{I}{A}}\frac{P^*h}{M^*}. \quad (39b)$$

Substituting the asymptotic expressions for the forces and moments from the post-buckling solution already presented, gives

$$P^* = \epsilon P^{*(1)} + \epsilon^2 P^{*(2)} + \ldots\ M^* = \epsilon M^{*(1)} + \epsilon^2 M^{*(2)} + \ldots \quad (40a)$$

where the first and second-order terms (i.e., $k = 1,2$) are (notice that the zero-order quantities in the expression for P^* cancel out)

$$P^{*(k)} = \frac{H}{T}P_d^{(k)} - \frac{h}{T}P_s^{(k)} - \frac{6hH}{T^3}M_b^{(k)}, \quad (40b)$$

$$M^{*(k)} = M_d^{(k)} - \frac{h^3}{T^3}M_b^{(k)}. \quad (40c)$$

In the previous relations, the first and second-order forces and moments, $P_d^{(k)}$, $P_s^{(k)}$, $M_d^{(k)}$, $M_b^{(k)}$, $k = 1, 2$ have already been found from the initial post-buckling solution described in the previous section.

Now the energy release rate and the Mode I and II stress intensity factors can be written in the form:

$$G = \epsilon^2 G^{(2)} + \epsilon^3 G^{(3)} + \ldots, \quad (41a)$$

$$K_{I,II} = \epsilon K_{I,II}^{(1)} + \epsilon^2 K_{I,II}^{(2)} + \ldots, \quad (41b)$$

where $K_{I,II}^{(1)}$, $K_{I,II}^{(2)}$ are found by substituting in (37) the first or second-order forces and moments, respectively, $G^{(2)}$ is found from (33) by substituting directly the first-order forces and moments and

$$G^{(3)} = \frac{1-\nu}{2\mu}\left[\frac{P^{*(1)}P^{*(2)}}{Ah} + \frac{M^{*(1)}M^{*(2)}}{Ih^3} + \frac{\sin\gamma}{\sqrt{AI}h^2}\left(P^{*(1)}M^{*(2)} + P^{*(2)}M^{*(1)}\right)\right]. \quad (41c)$$

Discussion of Results

The thin film model of Chai et al. (1981), which is a closed-form solution for the initial post-buckling and growth behavior, represents the limiting solution for a very large value of the ratio h/T, i.e., for a delamination in an infinitely thick base plate. This solution predicts an energy release rate

$$G(\epsilon_0, \ell) = \frac{1}{2}Eh(1-\nu^2)(\epsilon_0 - \epsilon_{cr})(\epsilon_0 + 3\epsilon_{cr}), \quad (42a)$$

where

$$\epsilon_{cr} = \frac{\pi^2 h^2}{12(1-\nu^2)\ell^2}, \quad (42b)$$

is the Euler's critical strain for the delaminated layer (treated as a column with built-in ends) and ϵ_0 is the applied strain. The applied load is $P = E\epsilon_0$ and the midpoint deflection is

$$w_{dm} = -\frac{4\ell}{\pi}\sqrt{(\epsilon_0 - \epsilon_{cr})(1-\nu^2)}. \quad (42c)$$

For this model, the mode mixity is given by the following relation (Hutchinson and Suo, 1991):

$$\tan\psi = \frac{4\cos\omega + \sqrt{3}\xi\sin\omega}{-4\sin\omega + \sqrt{3}\xi\cos\omega}. \quad (43a)$$

Since the thin film model postulates that $\eta = h/H - 0$, $\omega = 52.1^0$. Futhermore, ξ is defined by

$$\xi = \left[\frac{4}{3}\left(\frac{\epsilon_0}{\epsilon_{cr}} - 1\right)\right]^{1/2}. \quad (43b)$$

These results from the limiting thin film model are a very useful approximation and a comparison with the present general post-buckling solution is noteworthy. In applying the formulas presented in this paper, it should be remarked that in general, the critical end-amplitude for the delamination (that normally buckles with an inflection point) is $-\pi/2 > \Phi_d^0 > -\pi$ (the thin film model assumes $\Phi_d = -\pi$), whereas for the substrate part that normally shows no inflection point, $0 > \Phi_s^0 > -\pi/2$, and

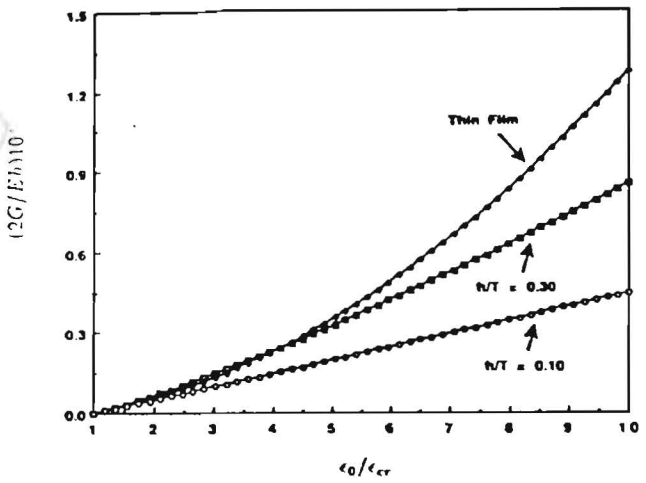

Fig. 2 Energy release rate, $(2G/Eh)10^5$, as a function of the applied strain

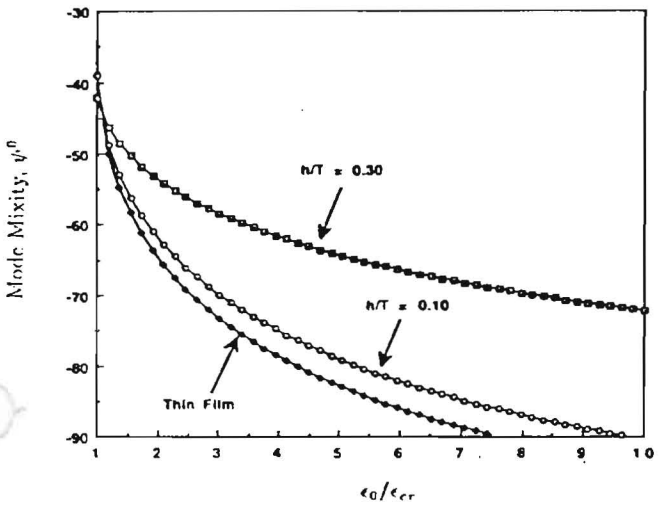

Fig. 3 Mode mixity, ψ^0, versus applied strain

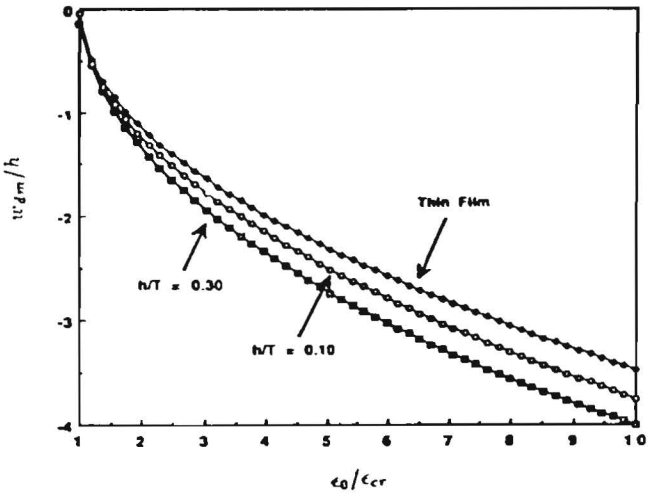

Fig. 4 Midpoint deflection of the delamination, w_{dm}/h, as a function of the applied strain

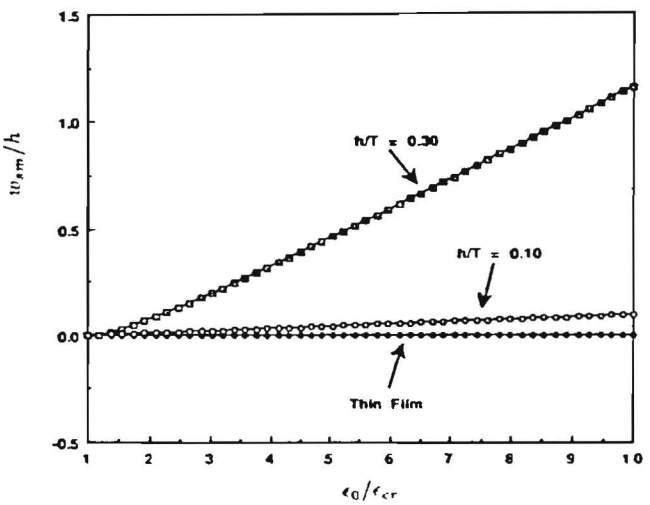

Fig. 5 Midpoint deflection of the substrate part, w_{sm}/h, versus applied strain

likewise for the base part, $\pi/2 > \Phi_b^0 > -\pi/2$. Moreover, the distortion parameter for the delamination is $\epsilon < 0$ (Fig. 1).

For an illustration of the results from the previous analysis consider a delaminated plate with $E = 10$ GPa and $\nu = 0.3$ and delamination and plate length $\ell = 20$ mm and $L = 60$ mm, respectively, and delamination thickness $h = 0.4$ mm. These dimensions correspond to our specimen dimensions (a width of 10 mm has been considered and is appropriately accounted in the results). To keep the critical strain ϵ_{cr} constant we keep the delamination length and thickness constant and vary only the plate thickness to get a varying ratio h/T; this would ensure the same thin film model solution.

Figure 2 shows the energy release rate $(2G/Eh)10^5$, as a function of the applied strain for $h/T = 0.10$ and $h/T = 0.30$. It is seen that for the same applied strain, the energy release rate for the case of the delamination located further away from the surface ($h/T = 0.3$) is always higher than the one for the delamination close to the surface ($h/T = 0.1$). In the beginning, i.e., for relatively small applied strain, the curves tend toward the thin film solution for a decreasing ratio h/T (as expected); however, as the applied strain is increased, the thin film model solution rises even above the $h/T = 0.3$ solution and predicts a much higher energy release rate. Experimental results that have been previously reported by Kardomateas (1989b, 1990) confirm clearly the reduced growth resistance of the "large ratio" case, $h/T = 0.3$, versus the "small ratio" one, $h/T = 0.1$). In fact, the small ratio delamination in these studies did not grow at all despite a very large increase in the applied strain. Notice that this important difference in growth behavior cannot obviously be predicted by the thin film model, which, because of its strongly nonlinearly increasing $G - \epsilon_0$ curve, would predict growth even for the small ratio delamination if the applied strain would be sufficiently increased.

Another very interesting result is the variation of the mode mixity (Mode II versus Mode I) at the delamination tip. Figure 3 shows the mode mixity ψ versus applied strain. It is seen that for the same applied strain the delamination located further away from the surface ($h/T = 0.3$) shows a higher mode I proportion than the one for the delamination close to the surface ($h/T = 0.1$). As a consequence, the value of the applied strain at which the delamination tip loading becomes pure Mode II ($\psi = -90$ deg) is increased. This point for the thin film model is at $\epsilon_0/\epsilon_{cr} = 7.55$. The curve show a trend toward the thin film solution for a decreasing ratio h/T.

Figure 4 shows the midpoint deflection of the delamination, w_{dm}/h, and Fig. 5 shows the midpoint deflection of the substrate part, w_{sm}/h, both as a function of the applied strain. It is seen that both curves show a trend toward the thin film solution for a decreasing ratio h/T and that the midpoint deflections are higher for a larger value of h/T (delaminations located further away from the surface).

Figure 6 shows the applied load P versus applied strain curves. It is seen that for the same value of applied strain, the delamination located further away from the surface ($h/t = 0.3$) exhibits a lower applied load and hence a larger loss of stiffness than the delamination close to the surface ($h/t = 0.1$). Again,

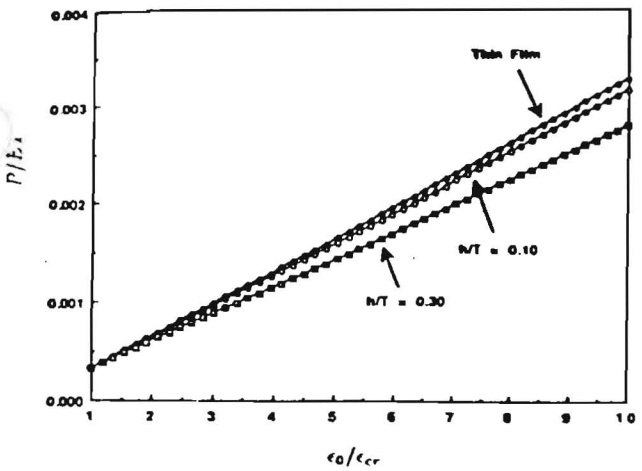

Fig. 6 Applied load P versus applied strain curves

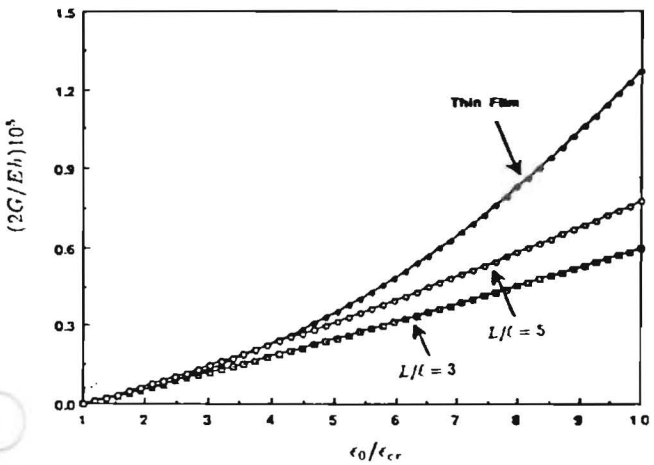

Fig. 7 Energy release rate as a function of the applied strain illustrating the effect of relative plate length

the curves tend to the thin film limit for a decreasing h/T value.

Next, the influence of the base plate length is studied by keeping the delamination length and thickness constant, and varying only the plate length to get a ratio L/ℓ of 3 and 5. In this example the plate thickness was chosen so that $h/T = 0.20$. This effect is mostly evident on the energy release rate, which is shown in Fig. 7 as a function of the applied strain. It is seen that the effect of plate length is evident at higher values of applied strain with the longer plate exhibiting higher energy release rates (and closer to the thin film solution).

Acknowledgment

The financial support of the Office of Naval Research, Mechanics Division, Grant N00014-91-J-1892, and the interest and encouragement of the Project Monitor, Dr. Y. Rajapakse, are both gratefully acknowledged.

References

Britvek, S. J., 1973, *The Stability of Elastic Systems*, Pergamon, New York.

Chai, H., Babcock, C. D., and Knauss, W. G., 1981, "One Dimensional Modelling of Failure in Laminated Plates by Delamination Buckling," *Int. J. Solids Structures*, Vol. 17, pp. 1069-1083.

Chai, H., and Babcock, C. D., 1985, "Two-Dimensional Modelling of Compressive Failure in Delaminated Laminates," *J. Comp. Mat.*, Vol. 19, pp. 67-

Chai, H., 1990, "Three-Dimensional Fracture Analysis of Thin Film Debonding," *Int. J. Fracture*, Vol. 46, pp. 237-256.

Dundurs, J., 1969, *Mathematical Theory of Dislocations*, ASME, New York, pp. 70-115.

Evans, A. G., and Hutchinson, J. W., 1984, "On the Mechanics of Delamination and Spalling in Compressed Films," *Int. J. Solids Structures*, Vol. 20, No. 5, pp. 455-466.

Hutchinson, J. W., and Suo, Z., 1992, "Mixed Mode Cracking in Layered Materials," *Advances in Applied Mechanics*, Vol. 29, Academic Press, New York, pp. 63-191.

Kardomateas, G. A., and Schmueser, D. W., 1988, "Buckling and Postbuckling of Delaminated Composites Under Compressive Loads Including Transverse Shear Effects," *AIAA Journal*, Vol. 26, pp. 337-343.

Kardomateas, G. A., 1989a, "Large Deformation Effects in the Postbuckling Behavior of Composites With Thin Delaminations," *AIAA Journal*, Vol. 27, pp. 624-631.

Kardomateas, G. A., 1989b, "Geometric Nonlinearities in the Postbuckling Behavior of Delaminated Composites," *Interlaminar Fracture in Composites* ("Key Engineering Materials," series), Trans. Tech. Publications, Switzerland, pp. 269-284.

Kardomateas, G. A., 1990, "Postbuckling Characteristics in Delaminated Kevlar/Epoxy Laminates: An Experimental Study," *Journal of Composites Technology and Research (ASTM)*, Vol. 12, No. 2, pp. 85-90.

Simitses, G. J., Sallam, S., and Yin, W. L., 1985, "Effect of Delamination on Axially Loaded Homogeneous Laminated Plates," *AIAA Journal*, Vol. 23, No. 9, pp. 1437-1444.

Storåkers, B., and Andersson, B., 1988, "Nonlinear Plate Theory Applied to Delamination in Composites," *J. Mech. Phys. Solids*, Vol. 36, No. 6, pp. 689-718.

Suo, Z., and Hutchinson, J. W., 1990, "Interface Crack Between Two Elastic Layers," *International Journal of Fracture*, Vol. 43, pp. 1-18.

Wang, S. S., Zahlan, N. M., and Suemasu, H., 1985, "Compressive Stability of Delaminated Random Short-Fiber Composites, Part I—Modeling and Methods of Analysis," *J. Comp. Mat.*, Vol. 19, pp. 296-316.

Yin, W. L., 1985, "Axisymmetric Buckling and Growth of a Circular Delamination in a Compressed Laminate," *Int. J. Solids Structures*, Vol. 21, pp. 503-514.

APPENDIX A

The constant c_1 in Eq. (28) is given as follows:

$$c_1 = \frac{D_d}{\ell} c_{1d} + \frac{D_s}{\ell} c_{1s} + \frac{D_b}{b} c_{1b} + c_{1c}, \tag{A1}$$

where

$$c_{1d} = \left(\frac{\Phi_d^0}{2}\cos\Phi_d^0 + \sin\Phi_d^0\right)\phi_d^{(1)2} - \frac{\Phi_d^0}{16}\cos\Phi_d^0\left(\frac{1}{3} - \frac{\sin 2\Phi_d^0}{2\Phi_d^0}\right), \tag{A2a}$$

$$c_{1s} = \alpha_s^{(1)}\left[\left(\frac{\Phi_s^0}{2}\cos\Phi_s^0 + \sin\Phi_s^0\right)\phi_s^{(1)2} - \frac{\Phi_s^0}{16}\cos\Phi_s^0\left(\frac{1}{3} - \frac{\sin 2\Phi_s^0}{2\Phi_s^0}\right)\alpha_s^{(1)2}\right] - (\cos\Phi_s^0 - \Phi_s^0\sin\Phi_s^0)\phi_s^{(1)}\alpha_s^{(2)} + \gamma_c\Phi_s^0\cos\Phi_s^0, \tag{A2b}$$

$$c_{1b} = -q(\alpha_b^{(1)}\rho_c + \phi_b^{(1)}\alpha_b^{(2)}) - \left(\Phi_b^0 + \frac{\pi}{2}\right)\cos\Phi_b^0 \times\left[\eta_c + \left(\frac{1}{3} - \frac{\sin 2\Phi_b^0}{2[\Phi_b^0 + (\pi/2)]}\right)\frac{\alpha_b^{(1)3}}{16}\right] + \left[\sin\Phi_b^0 + \left(\Phi_b^0 + \frac{\pi}{2}\right)\frac{\cos\Phi_b^{(1)}}{2}\right]\phi_b^{(1)2}\alpha_b^{(1)}, \tag{A2c}$$

and

$$c_{1c} = \left[\left(\frac{\sin 2\Phi_s^0}{\Phi_s^0} - 2\cos 2\Phi_s^0\right)\frac{\phi_s^{(1)}\alpha_s^{(1)2}}{4\Phi_s^0} + \left(1 - \frac{\sin 2\Phi_s^0}{2\Phi_s^0}\right)\alpha_s^{(1)}\alpha_s^{(2)} - \left(\frac{\sin 2\Phi_d^0}{\Phi_d^0} - 2\cos 2\Phi_d^0\right)\frac{\phi_d^{(1)}}{4\Phi_d^0} - \frac{\psi_c T}{\ell}\right]\frac{EhH}{4} \tag{A2d}$$